JOURNAL OF COMPUTATIONAL PHYSICS 58, 417–431 (1985)

An Implicit Scheme for Efficient Solution of the Coalescence/Collision-Breakup Equation

PHILIP S. BROWN, JR.

The Center for the Environment and Man, Inc.,
275 Windsor Street, Hartford, Connecticut 06120

Received August 24, 1983; revised April 10, 1984

Detailed moist-convection models of the atmosphere require solution of the coalescence/collision-breakup equation to predict change in the water-drop spectrum. Under certain meteorological conditions, computational stability problems are encountered in attempting to solve this equation by explicit techniques. A stability analysis is performed making use of empirical results that depend on the form of observed drop spectra and the nature of the equation. Information derived from the analysis is used to design a two-step implicit scheme that provides both stability and efficiency.

1. INTRODUCTION

In modeling moist atmospheric convection, cloud microphysics equations governing water-drop size must be solved in conjunction with equations governing macrophysical processes such as convection of heat and momentum. Under certain physical conditions, the time constants associated with the microphysics are much smaller than those associated with the convection process (e.g., [1, 2]). Due to the disparity of the time constants, the combined set of equations constitutes a stiff system and special numerical techniques are required to solve the system in an efficient manner.

In this paper we consider the integro-differential (microphysics) equation describing the rate of change of the water-drop spectrum due to the simultaneous action of coalescence and collision-induced breakup. For this composite equation we examine the mechanisms that give rise to small time constants thereby extending earlier work in which the coalescence and breakup processes were considered separately and in different algorithmic settings [2, 3]. When these mechanisms are at work, explicit solution techniques require the use of small time increments to maintain computational stability. Such explicit procedures are commonly used but are not well suited to the problem. As an alternative, we present an efficient implicit scheme designed to allow the use of large time increments commensurate with those typically used to treat the macrophysical processes. The truncation error produced by expansion of the time increment is considered and found to be acceptably small. Incorporation of the new scheme in moist convection models eliminates the need to

0021-9991/85 $3.00

use different temporal grids for different processes and eliminates the risk of computational instability.

2. The Coalescence/Breakup Equation

The coalescence/breakup equation is given by Gillespie and List [4] as

$$\frac{\partial n(m)}{\partial t} = \mathscr{B} + \mathscr{C} \tag{1}$$

where

$$\mathscr{B}(m) = \int_0^\infty \int_0^\mu n(\mu)\, n(\mu_1)\, f(\mu, \mu_1)\, P(m; \mu, \mu_1)\, d\mu_1\, d\mu$$
$$- \int_0^\infty \frac{1}{m+\mu_1} \int_0^{m+\mu_1} \mu n(m)\, n(\mu_1)\, f(m, \mu_1)\, P(\mu; m, \mu_1)\, d\mu\, d\mu_1 \tag{2}$$

and

$$\mathscr{C}(m) = \int_0^{m/2} n(\mu)\, n(m-\mu)\, f(\mu, m-\mu)\, E_2(\mu, m-\mu)\, d\mu$$
$$- \int_0^\infty n(m)\, n(\mu)\, f(\mu, m)\, E_2(\mu, m)\, d\mu. \tag{3}$$

The definitions for the quantities appearing in (2) and (3) are

$n(m)$ = number density for drops of mass m,
t = time,
$E_2(\mu, \mu_1)$ = coalescence efficiency for drops of masses μ, μ_1,
$P(m; \mu, \mu_1)$ = mean number of fragments of mass m per collision resulting from breakup of drops with masses μ, μ_1 ($\mu \geqslant \mu_1$),
$f(\mu, \mu_1) = \pi(r_\mu + r_{\mu_1})^2 E_1(\mu, \mu_1)\, |\Delta V(\mu, \mu_1)|$,
r_μ = radius of a drop of mass μ,
$E_1(\mu, \mu_1)$ = collision efficiency for drops of masses μ, μ_1,
$\Delta V(\mu, \mu_1)$ = difference in terminal velocities for μ and μ_1 drops.

In (3) the coalescence integrals are not written in traditional form, and it is well to point out that the "collection efficiency" ($E_1 \times E_2$) appears implicitly through the product

$$K = f \times E_2, \tag{4}$$

commonly referred to as the "collection kernel." In the above expressions, $\mathscr{B}$ represents the terms corresponding to collision breakup and $\mathscr{C}$ the terms corresponding to coalescence. For notational convenience, the dependence of n, $\mathscr{B}$, and $\mathscr{C}$ on t is suppressed. In this study we restrict consideration to drops having mean diameter >0.14 mm and thereby disregard any effects of small-sized cloud droplets. In this framework the collision efficiency E_1 is taken to be unity based upon the experiments of McTaggart–Cowan and List [5]. Their experiments showed that for larger drops (viz., raindrops), the "geometric" value of unity is appropriate since the drop trajectories are essentially undisturbed by the flow field around the drops [4]. Earlier results for smaller droplet pairs (especially cloud droplets) have shown $E_1 < 1$ (e.g., Levin *et al.* [6]). In conformance with [4], the coalescence efficiency is expressed in the form suggested by Whelpdale and List [7] but modified to include the more recent experimental results of McTaggart–Cowan and List who observed no coalescence for drops with $r_{\mu_1} \geqslant 0.5$ mm. Due to lack of available information, E_2 is taken to be zero in the band, $0.25 \text{ mm} < r_{\mu_1} < 0.5$ mm. Thus, we set

$$\begin{aligned} E_2(\mu, \mu_1) &= (1 + r_{\mu_1}/r_\mu)^{-2}, \qquad r_{\mu_1} \leqslant 0.25 \text{ mm}, \\ &= 0, \qquad\qquad\qquad \text{otherwise.} \end{aligned} \tag{5}$$

To calculate the terminal velocity V_T of a raindrop of mass μ, we use the formula of Best [8] for low-altitude calculations,

$$V_T(\mu) = A\{1 - \exp[-(\mu/a)^p]\}, \tag{6}$$

where $A = 9.32 \text{ msec}^{-1}$, $a = 2.9$ mg and $p = 0.382$ (μ given in mg).

The fragment distribution function P can be written as

$$P(m; \mu, \mu_1) = P_L(m; \mu, \mu_1) + P_s(m; \mu, \mu_1) \tag{7}$$

where P_L and P_s are the large-drop and small-drop distributions, respectively [4]. P_L is a partial Gaussian distribution of the form

$$\begin{aligned} P_L(m; \mu, \mu_1) &= H \exp[-(m-\mu)^2/(2\sigma^2)], \qquad \text{if} \quad m \leqslant \mu + \mu_1, \\ &= 0, \qquad\qquad\qquad\qquad\qquad\quad \text{otherwise,} \end{aligned} \tag{8}$$

with

$$H = 11.8/[d_L^4\, d_s(0.41 - 0.30 d_s/d_L)]. \tag{9}$$

Here $d_L = 2r_\mu$ and $d_s = 2r_{\mu_1}$, the resective large- and small-drop diameters in millimeters; σ ($\approx H^{-1}$) is the standard deviation. The small drop distribution takes the form

$$\begin{aligned} P_s(m; \mu, \mu_1) &= (6.0\bar{f}/d_s)(m/0.065)^\alpha, \qquad \text{if} \quad m \leqslant 1 \text{ mg}, \\ &= (6.0\bar{f}/d_s)\, m^{-2.6}/0.0654^\alpha, \quad \text{otherwise,} \end{aligned} \tag{10}$$

where

$$\alpha = -1.0 - 0.392/d_s \tag{11}$$

and $\bar{f}$, the mean number of small fragments, is

$$\bar{f} = 3.6(d_L^3\, d_s)^{1/2}(0.41 - 0.30 d_s/d_L). \tag{12}$$

As a first step in the solution of (1), the mass coordinate is discretized by choosing an expanding set of grid points $m_1, m_2, ..., m_{N+1}$ where for convenience we let $m_{i+1} = 2m_i$ (with $m_1 = 0.00102$ mg). The expanding grid provides high resolution at the lower end of the spectrum where coalescence substantially alters the otherwise exponentially decreasing drop distribution. The mass discretization allows (1) to be represented as an autonomous system of nonlinear ODEs with time as the independent variable. Instead of directly replacing the integrals in (2) and (3) by quadrature formulas, however, we adopt a special technique due to Bleck [9]. The procedure is designed to preserve total liquid water content of the droplet spectrum and to provide an efficient algorithm by allowing much of the computation to be performed in one initial set of calculations.

To implement the Bleck method, we average (1) over each mass interval $[m_i, m_{i+1}]$ and define the mean number density n_i over that interval as

$$n_i = \frac{\int_{m_i}^{m_{i+1}} n(m)\, m\, dm}{\int_{m_i}^{m_{i+1}} m\, dm}. \tag{13}$$

After the averaging operation is performed on (1), the functions n appearing in the integrands of $\mathscr{B}$ and $\mathscr{C}$ are approximated by appropriate averages n_i. The domains of integration are partitioned into subregions in each of which the mean number density is assumed constant and hence can be taken outside the integral. The resulting integrals then do not involve the dependent variable and can be evaluated once and for all. These integrals are represented by the coefficients in the quadratic forms that appear in the resulting system

$$\frac{dn_i}{dt} = B_i + C_i, \qquad i = 1, ..., N \tag{14}$$

where

$$B_i = \frac{2}{m_{i+1}^2 - m_i^2}\left(\sum_{j=1}^{N}\sum_{k=1}^{j} p_{ijk} n_i n_k - n_i \sum_{k=1}^{i} q_{ik} n_k\right) \tag{15}$$

and

$$C_i = \frac{2}{m_{i+1}^2 - m_i^2}\left(\sum_{j=i-1}^{i}\sum_{k=1}^{i-1} a_{ijk} n_j n_k - n_i \sum_{k=1}^{N} b_{ik} n_k\right). \tag{16}$$

$\mathbf{B} = (B_i)$ and $\mathbf{C} = (C_i)$ are the vectors corresponding to the breakup and coalescence terms in (1).

The Bleck coalescence coefficients are given by integrals of the collection kernel K as

$$a_{ijk} = \int_{A_{ijk}} K(\tilde{\mu}, \mu)(\tilde{\mu} + \mu)\, d\tilde{\mu}\, d\mu \tag{17}$$

and

$$b_{ik} = \int_{B_{ik}} K(m, \mu)\, m\, dm\, d\mu \tag{18}$$

where $\tilde{\mu}$ represents $m - \mu$ and the domains of integration are described by

$$A_{ijk} = \{(\tilde{\mu}, \mu): \max(m_j, m_i - \mu, \mu) \leqslant \tilde{\mu} \leqslant \min(m_{j+1}, m_{i+1} - \mu) \text{ and } m_k \leqslant \mu \leqslant m_{k+1}\} \tag{19}$$

and

$$B_{ik} = \{(m, \mu): m_i \leqslant m \leqslant m_{i+1} \text{ and } m_k \leqslant \mu \leqslant m_{k+1}\}. \tag{20}$$

The somewhat complicated inequalities defining the A_{ijk}'s are an algebraic description of a simple partition of the triangular region, $m_1 \leqslant \tilde{\mu} \leqslant m_{N+1}$; $m_1 \leqslant \mu \leqslant \tilde{\mu}$, into smaller polygonal areas in each of which the number densities $n(\mu)$, $n(\tilde{\mu})$ are assumed constant [9, 10].

The breakup coefficients take the form [11]

$$p_{ijk} = \int_{C_{ijk}} m(\mu^{1/3} + \mu_1^{1/3})^2 U(m; \mu, \mu_1)\, d\mu_1\, d\mu\, dm \tag{21}$$

and

$$q_{ik} = \int_{D_{ik}} \frac{m\mu}{(m + \mu_1)} (m^{1/3} + \mu_1^{1/3})^2 U(\mu; m, \mu_1)\, d\mu_1\, d\mu\, dm \tag{22}$$

where

$$U(m; \mu, \mu_1) = (3/4)^{2/3} \pi^{1/3} \rho_w^{-2/3} E_1(\mu, \mu_1)\, |\Delta V(\mu, \mu_1)|\, P(m; \mu, \mu_1), \tag{23}$$

with ρ_w the water density, and where

$$C_{ijk} = \{(m, \mu, \mu_1): m_i \leqslant m \leqslant m_{i+1}; m_j \leqslant \mu \leqslant m_{j+1}; m_k \leqslant \mu_1 \leqslant m_{k+1}\} \quad \text{for } k < j \tag{24}$$

$$C_{ijj} = \{(m, \mu, \mu_1): m_i \leqslant m \leqslant m_{i+1}; m_j \leqslant \mu \leqslant m_{j+1}; m_j \leqslant \mu_1 \leqslant \mu\} \tag{25}$$

$$D_{ik} = \{(m, \mu, \mu_1): m_i \leqslant m \leqslant m_{i+1}; m_1 \leqslant \mu \leqslant m_{N+1}; m_k \leqslant \mu_1 \leqslant m_{k+1}\}. \tag{26}$$

Pitfalls in evaluating the integral (21) are discussed in [12]. The complexity of the formulas precludes simple characterization of the coefficient behavior as a function of index. However, we can note, at least, that for fixed i, local maxima occur in the arrays p_{ijk} for $j = i$, $k = i - 1$ resulting from the Gaussian peak in P_L; largest values occur for $j = N$, $k = N - 3$ to N corresponding to the collision of pairs of very large

drops. For $N = 17$, the wide range in magnitude of the matrix elements is illustrated for $i = 6, 12$:

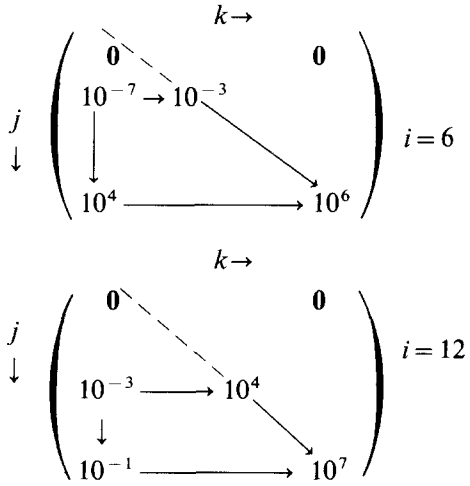

The q_{ik}'s are evaluated by taking appropriate sums of the p_{ijk}'s weighted by the factor $m/(m+\mu_1)$. It is shown later how the breakup terms, rather than the coalescence terms, are responsible for the computational stability problem under investigation.

3. The Stability Problem

Takahashi [13, 14], in a pioneering effort to include the collision-breakup process in a moist-convection model, reported computational difficulties. Takahashi used an explicit (forward-stepping) solution procedure and found that an exceedingly small step size (1s) was required to maintain computational stability. The reported problem led to a stability analysis of the breakup equation [2] formulated using standard finite-difference approximations that preserve neither drop number nor water mass. The analysis led to the discovery of both physical and computational mechanisms capable of inducing the stability problem encountered by Takahashi. We now apply the same type of analysis to the combined coalescence collision-breakup equation (14) and, using information derived from the analysis, design a stable scheme.

As a first step, we linearize the right-hand side of (14) using a truncated Taylor expansion to obtain an approximation that lends itself to analysis. The inhomogeneous terms can be neglected since only the homogeneous terms affect stability [15]. Thus a time-differencing scheme to be used for (14) is analyzed for stability by applying the scheme to the test equation

$$\frac{d\mathbf{n}}{dt} = \mathbf{A}\mathbf{n} \tag{27}$$

where $\mathbf{n} = (n_1, n_2, \ldots, n_N)^{\mathrm{T}}$ and where $\mathbf{A} = (\alpha_{ij})$ is the Jacobian matrix that arises from the linearization of **B** and **C**. If we expand about the point $t = t_0$, then $\mathbf{A}(\mathbf{n})$ is evaluated at t_0. Since the approximation is valid only for short ranges of t, **A** must be updated during the course of the step-by-step solution process. We assume that **A** is diagonalizable so that the stability conditions for the numerical integration of (27) are the same as those for the N independent equations

$$\frac{d\nu_i}{dt} = \lambda_i \nu_i \tag{28}$$

where the λ_i are the eigenvalues of **A** (e.g., [15]).

The general functional form for $\mathbf{A}(\mathbf{n})$ is complicated and provides little insight into the nature of the λ_i required to treat the stability problem. Nevertheless, if n is assumed to have "Marshall–Palmer" exponential form, typical of observed drop spectra, numerical evaluation of $\mathbf{A}(\mathbf{n})$ suggests that the λ_i may be identified immediately, and further that the λ_i can be expressed in closed analytical form. The Marshall–Palmer form is

$$n(d) = N_0 e^{-\Lambda d} \tag{29}$$

where d denotes drop diameter and N_0, Λ are constants. If (29) is chosen for the initial distribution, the solution of (14) remains nearly exponential (though Λ, N_0 change) except at small values of d where coalescence has a pronounced effect. Throughout the evolution of the spectrum, **A** remains approximately upper triangular due to the special nature of the spectrum and the Bleck coefficients. (Elements below the main diagonal are nonzero but relatively small.) Such a form suggests that the eigenvalues of **A** are close to its diagonal elements. In (30) we sketch the form of **A** for a typical drop distribution, where the fixed-point values have been rounded to two decimal places.

$$A = \left[\begin{array}{ccccccccc}
-.04 & .00 & & & \cdots & & -.25 & & -.83 \\
.00 & -.04 & \ddots & & & & & & \vdots \\
 & \ddots & .00 & -.02 & & & & & -6.55 \\
\hline
 & & .00 & .00 & -.03 & & & & \sim 10^4 \\
 & & & .00 & .01 & -.05 & & & \vdots \\
 & & & & & \ddots & -.30 & & .20 \\
 & & & & & & .00 & -.43 & 1.05 \\
 & & \multicolumn{2}{c}{|\alpha_{ij}| < \mathbf{.005}} & & & & .00 & -.63
\end{array}\right]. \tag{30}$$

Even though the matrix is approximately upper triangular, the diagonal elements

may not provide a good approximation to the eigenvalues as we may see by considering the simple 2×2 form (as suggested by one of the reviewers)

$$\begin{pmatrix} 1 & 10^5 \\ 4 \times 10^{-5} & 4 \end{pmatrix}.$$

Here the eigenvalues are 0 and 5 and not the diagonal entries 1 and 4. As for the 2×2 example, **A** contains upper triangular elements many orders of magnitude larger than the lower triangular elements. Thus it is possible for products of the lower triangular elements with upper triangular elements to affect significantly the coefficients (and roots) of the characteristic equation, so that the A_{ii} might not provide an adequate representation of the λ_i.

To check against this possibility, we have computed the eigenvalues of **A** by the QR method (e.g., [16]) in which **A** is iteratively transformed to more nearly exact upper triangular form. The first step involves direct transformation of **A** to an upper Hessenberg matrix **H** ($H_{ij} = 0$ for $j \leqslant i-2$). Calculations show that the upper triangular elements of **H** are not increased (but actually decreased) relative to the lower triangular elements. The QR method then reduces the subdiagonal elements $H_{i,i-1}$ to "machine ε" relative to the diagonal elements. For all cases tested (including those listed in Table I), the calculations verify that the diagonal elements of **A** are, in fact, close approximations to the eigenvalues. The diagonal elements are nonpositive and, except where coalescence has a small effect, increase in magnitude as we move down the diagonal. Thus $|\alpha_{ii}| > |\alpha_{jj}|$, where $i > j$ so that α_{NN} is the dominant (negative) eigenvalue $\lambda_{\mathscr{D}}$ given by the simple expression

$$\lambda_{\mathscr{D}} = \alpha_{NN} = \frac{\partial}{\partial n_N}(B_N + C_N). \tag{31}$$

As a consequence of this result, if larger drop categories ($> m_{N+1}$) are included in the model, $|\lambda_{\mathscr{D}}|$ will be increased accordingly. Due to the cutoff in the coalescence efficiency (5), C_N has no direct effect in (1), and $|\lambda_{\mathscr{D}}|$ represents the net rate at which drops of mass m_N are lost due to collision breakup alone. However, coalescence has indirect influence on $\lambda_{\mathscr{D}}$ since the process affects the spectrum **n** upon which B_N depends.

For explicit time-differencing schemes, it is $\lambda_{\mathscr{D}}$ that determines computational stability. As an example, the Euler method applied to (14) can be written in vectorized form

$$\mathbf{n}^{\tau+1} - \mathbf{n}^{\tau} = \Delta t(\mathbf{B} + \mathbf{C})^{\tau}, \tag{32}$$

where $\mathbf{n}^{\tau}$ is the finite-difference approximation to $\mathbf{n}(t)$ at $t = \tau \Delta t$, $\tau = 0, 1, 2, \ldots$, and where $(B + C)^{\tau} = B(\mathbf{n}^{\tau}) + C(\mathbf{n}^{\tau})$. Linearization yields

$$\mathbf{n}^{\tau+1} - \mathbf{n}^{\tau} = \Delta t\, \mathbf{A}\mathbf{n}^{\tau}. \tag{33}$$

The stability criterion for (33) is found by consideration of the equivalent system

$$v_i^{\tau+1} = (1 + \Delta t \lambda_i)\, v_i^{\tau}, \qquad i = 1,..., N. \tag{34}$$

Equation (34) is stable if, and only if, $|1 + \Delta t \lambda_i| \leqslant 1$ for each i. For the case in which the λ_i are negative, it follows that the criterion for stability is $\Delta t \leqslant \Delta t_c$, where

$$\Delta t_c = \frac{2}{|\lambda_{\mathscr{D}}|} \tag{35}$$

so that a large $|\lambda_{\mathscr{D}}|$ severely restricts the allowable step size. The "time constants" for the system are defined to be the $-1/\lambda_i$, so that $|\lambda_{\mathscr{D}}|^{-1}$ is the "fastest" time constant.

Table I lists values of $\lambda_{\mathscr{D}}$ and Δt_c for several exponential drop distributions of the form $N_0 e^{-\Lambda d}$. R denotes the rainfall rate associated with the given distribution. For the last case shown, the Euler method would require a time increment of about 1 sec to ensure stability. It is seen that an increase in N_0 or R produces a smaller value of Δt_c. The maximum rainfall rate considered here is 200 mm hr^{-1}, a value which represents an extreme situation but one that can occur locally in tropical convective activity. To be acceptable, a solution algorithm should be able to deal effectively with situations involving very heavy rainfall.

In the context of moist convection modeling, the time increments associated with the last three cases in Table I are undesirably small when used in parallel with values of Δt from 15 to 30 sec, say, to integrate the convection equations. Figures 1a,b illustrate results obtained with $N_{00}[= N_0(t=0)]$ set to 8×10^{-4} mm^{-4} and $\Lambda = 4.1$ (implying a rainfall rate $R = 100$ mm hr^{-1}). Figure 1a shows the evolution of the spectrum computed using (32) with a time increment of 2 sec; Fig. 1b shows the development of instability when Δt ($=4$ sec) slightly exceeds Δt_c. The insets show the variation in time of the critical time increment Δt_c computed from (31) and (35). The behavior of Δt_c versus t is significantly different from that presented in [2] due to the substantial difference in the evolution of the spectrum due to the incorporation of coalescence and the use of Bleck's mass-conserving scheme. When the "classical value" of $N_{00} = 8 \times 10^{-6}$ mm^{-4} is used with

TABLE I

Dominant Eigenvalue of A and Corresponding Δt_c for Drop Distributions of the Form $N_0 e^{-\Lambda d}$

N_0 (mm^{-4})	Λ (mm^{-1})	R (mm hr^{-1})	$\lambda_{\mathscr{D}}$ (sec^{-1})	Δt_c (sec)
8×10^{-6}	1.56	100	−0.05	37.94
8×10^{-4}	4.10	100	−0.68	2.96
8×10^{-4}	3.55	200	−0.97	2.05
2×10^{-3}	4.30	200	−1.50	1.34

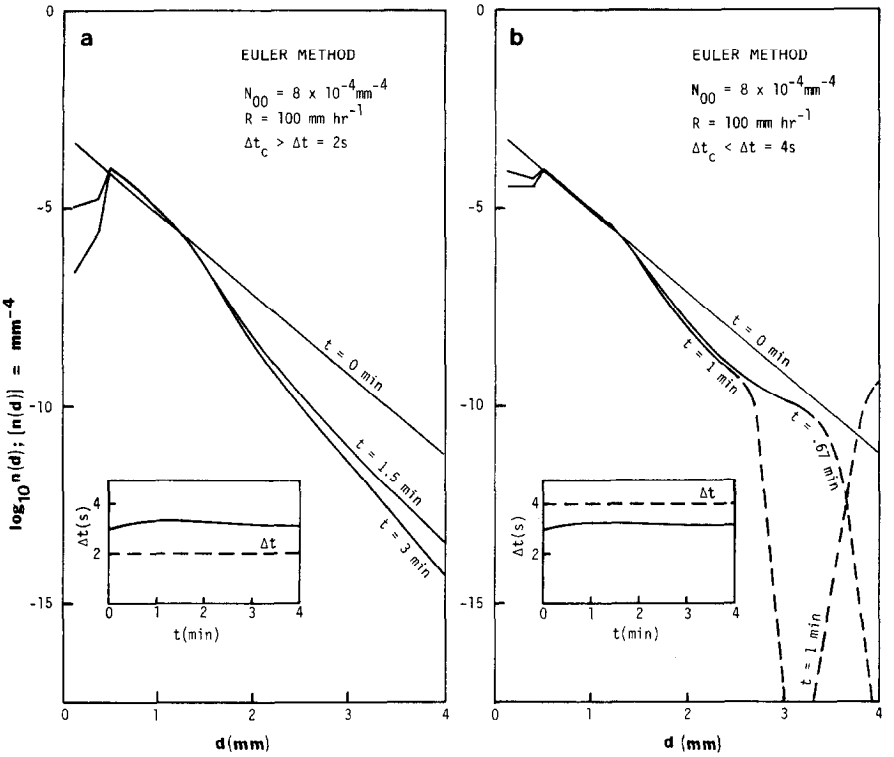

FIG. 1. Time evolution through breakup and coalescence of water drop spectra initially of Marshall–Palmer Form $n(d) = N_{00} \exp(-\Lambda d)$ with rainfall rate R computed using the explicit Euler method with time increment Δt for $N_{00} = 8 \times 10^{-4}$ mm^{-4} and $R = 100$ mm hr^{-1}. Solution is stable in (a), unstable in (b) for the values of Δt indicated. Dashed lines indicate positive $n(d)$ in the error-dominated portion of the spectrum where alternating positive and negative values occur for large d. Insets show Δt_c versus t (solution stable if and only if $\Delta t \leqslant \Delta t_c$); dashed lines in insets indicate values of Δt used in numerical solution.

$\Lambda = 1.56$ mm^{-1}, the restriction on Δt is less severe. Results for this case are shown in Figs. 2a,b, where it is seen that stability can be maintained with a Δt as large as 6 sec.

4. A Proposed Solution Technique

Simply maintaining stability of (32) through imposition of the stability criterion is safe but not efficient, and so we seek a scheme that offers unconditional stability without excessive computational burden. We consider the backward Euler method

$$\mathbf{n}^{\tau+1} - \mathbf{n}^{\tau} = \Delta t(\mathbf{B} + \mathbf{C})^{\tau+1} \tag{36}$$

which is stable for all $\Delta t > 0$. Due to the nonlinearity of **B** and **C**, (36) must be solved by iterative means, e.g., predictor–corrector schemes. However, convergence

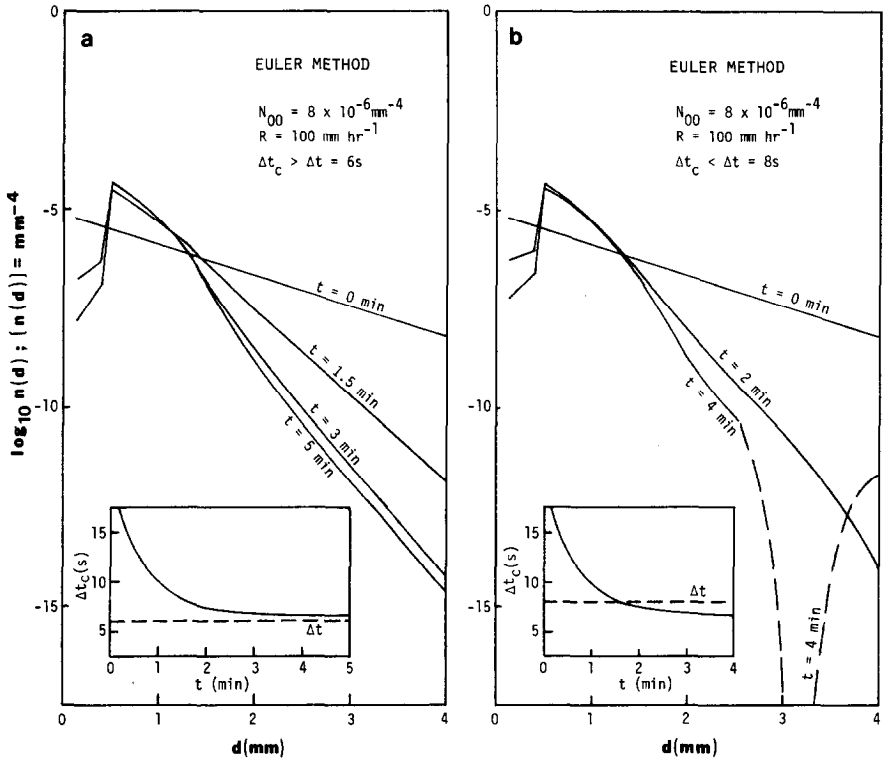

FIG. 2. Same as for Fig. 1 but with $N_{00} = 8 \times 10^{-6}\,\mathrm{mm}^{-4}$ (the "classical" value of N_{00}).

of standard corrector iteration formulas is controlled by the size of $|\lambda_{\mathscr{D}}|$ and again, for certain drop spectra, Δt has to be severely restricted to arrive at a solution. Newton-type iteration may be used, but this approach involves the added expense of evaluating the Jacobian matrix at possibly frequent intervals. The number of such evaluations can be reduced if the Jacobian elements vary slowly (e.g., Gear [17]). In moist-convection modeling, the Jacobian may vary slowly at some points in the spatial domain, but rapidly at others (e.g., where the liquid water content of the cloud is high). To avoid the problems associated with the nonuniformity of the convective-cloud domain in regard to rain formation, it is advantageous to design an algorithm that can be applied in exactly the same manner at every point.

To avoid the restriction on Δt, we design a convergent iteration using the fact that **A** is approximately upper triangular. Since it is the diagonal elements (the eigenvalues) of **A** that cause the stability problem, only those elements are involved in the terms that make the process implicit. Our algorithm is based on the scheme

$$n_i^* - n_i^\tau = \Delta t[B_i(n_1^\tau, \ldots, n_{i-1}^\tau, n_i^*, n_{i+1}^\tau, \ldots, n_N^\tau) + C_i(n_1^\tau, \ldots, n_{i-1}^\tau, n_i^*, n_{i+1}^\tau, \ldots, n_N^\tau)] \tag{37a}$$

$$n_i^{\tau+1} - n_i^{\tau} = \Delta t[B_i(n_1^*,..., n_{i-1}^*, n_i^{\tau+1}, n_{i+1}^*,..., n_N^*) + C_i(n_1^*,..., n_{i-1}^*, n_i^{\tau+1}, n_{i+1}^*,..., n_N^*)]. \quad (37b)$$

B_i and C_i are quadratic forms, so that all terms $n_i n_j$ are linear in n_i as long as $i \neq j$. Terms of the form n_i^2 we write as $n_i n_i^*$ in (37a) and $n_i^* n_i^{\tau+1}$ in (37b). This minor change in (37a), (37b) yields two sets of equations that are uncoupled and linear in the unknowns, and hence rapidly solvable. Based on (15), for example, (37b) is modified to

$$n_i^{\tau+1} - n_i^{\tau} = \frac{2\Delta t}{m_{i+1}^2 - m_i^2}\left\{\sum_{j=1}^{i-1} n_j^* \sum_{k=1}^{j} p_{ijk} n_k^* + n_i^{\tau+1} \sum_{k=1}^{i} p_{iik} n_k^* + \sum_{j=i+1}^{N} n_j^* \left(\sum_{\substack{k=1 \\ k\neq i}}^{j} p_{ijk} n_k^* + p_{iji} n_i^{\tau+1}\right) - n_i^{\tau+1} \sum_{k=1}^{i} q_{ik} n_k^* + \text{coalescence terms}\right\}. \quad (38)$$

Equations (37a), (37b) represent the first two steps of an iterative process whose rate of convergence can be estimated by applying the scheme to the linearized system (27). This version of the iteration takes the form

$$\mathbf{n}_{[l+1]}^{\tau+1} - \mathbf{n}^{\tau} = \Delta t[(\mathbf{A}-\mathbf{D})\mathbf{n}_{[l]}^{\tau+1} + \mathbf{D}\mathbf{n}_{[l+1]}^{\tau+1}], \qquad l = 0, 1, 2,..., \quad (39)$$

where $\mathbf{D}$ is the diagonal matrix containing the (negative) diagonal elements of $\mathbf{A}$. For analysis sake, (39) can be written as

$$\mathbf{n}_{[l+1]}^{\tau+1} = [(\mathbf{I}-\Delta t\mathbf{D})^{-1}\Delta t(\mathbf{A}-\mathbf{D})]\, n_{[l]}^{\tau+1} + (\mathbf{I}-\Delta t\mathbf{D})^{-1}\mathbf{n}^{\tau}. \quad (40)$$

Since $\mathbf{A}-\mathbf{D}$ is approximately upper triangular with zeros on the diagonal, the matrix product $\mathbf{P}$ inside the brackets [ ] has the same property, so that the eigenvalues of $\mathbf{P}$ are expected to be close to zero.

Since $\mathbf{P}$ is only an approximation to an upper triangular matrix, it is necessary to test computationally whether the eigenvalues of $\mathbf{P}(\Delta t)$ are, in fact, "close to zero"

TABLE II

Dominant Eigenvalue of $\mathbf{P}(\Delta t)$ for Drop Distributions of the form $N_0 e^{-\Lambda d}$

N_0 (mm^{-4})	Λ (mm^{-1})	R (mm hr^{-1})	$\lvert\lambda_2'\rvert$ (sec^{-1})
8×10^{-6}	1.56	100	0.44
8×10^{-4}	4.10	100	0.46
8×10^{-4}	3.55	200	0.56
2×10^{-3}	4.30	200	0.61

for the large Δt that we wish to use in practice. For this purpose, a value of $\Delta t = 15$ sec has been used in calculating the dominant eigenvalue $\lambda'_{\mathscr{D}}$ of $\mathbf{P}(\Delta t)$ by the QR method. The results are shown in Table II for the same exponential distributions treated in Table I. In each case, the eigenvalue largest in modulus (the "convergence factor") is not $\ll 1$ but at least is small enough to provide sufficiently rapid convergence. In principle, the iterative process should be continued until some suitable acceptability criterion is satisfied. In practice, we have found for all of the test cases listed in Table II, that if (37a), (37b) are followed by a third iteration, there is little change in the solution. In the worst case (largest $|\lambda'_{\mathscr{D}}|$), the change is at most 4% in the early stages of drop evolution ($t < 1$ min) and is $< 1\%$ in the later stages as the solution rapidly approaches equilibrium.

Figure 3 shows the results of applying the two-step scheme to the same problem whose solutions are illustrated in Fig. 1. The solid curves show the evolution of the spectrum using a 2 sec time increment used to maintain stability of the explicit scheme. The dashed curves show the solution computed with a time increment of 15 sec, commensurate with that appropriate for macrophysics processes. For the case treated here, Δt is substantially increased (by a factor of 7.5) without introducing unacceptably large truncation error. The error is confined mainly to the tails of the spectra which contain only about 2% of the total water content.

Figure 4 shows the solution curves for the "classical" case treated in Fig. 2. The truncation error brought about by the expansion of Δt from 6 to 15 sec is negligible for modeling purposes. In using the implicit scheme with $t = 15$ sec, we slightly

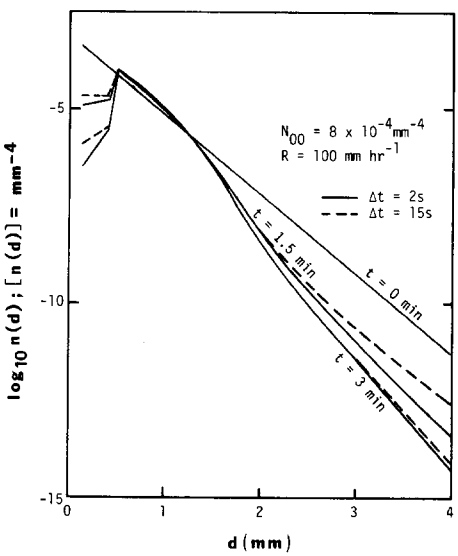

FIG. 3. Same case presented in Figs. 1a,b but with solution computed using the two-step implicit method. Solutions are generated with time increment $\Delta t = 2$ sec (solid curves) and 15 sec (dashed curves).

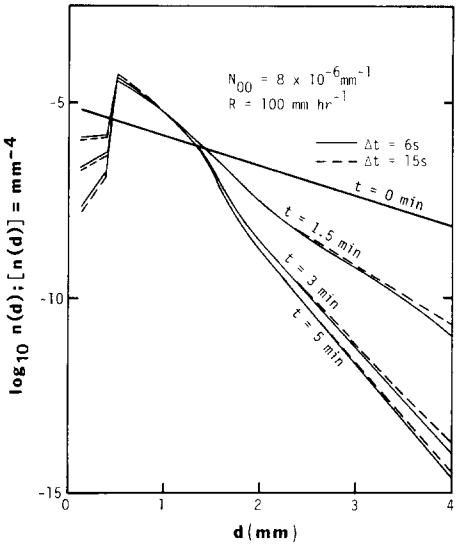

FIG. 4. Same case presented in Figs. 2a,b but with solution computed using the two-step implicit method. Solutions are generated with time increment $\Delta t = 6$ sec (solid curves) and 15 sec (dashed curves).

more than double the number of arithmetic operations per step and slightly more than double the step size so that there is no direct gain in efficiency over the explicit scheme. However, the need to compute eigenvalues and perform stability tests is eliminated.

Table III shows values of the ratio

$$R_{\text{CPU}} = \frac{\text{CPU time (sec) for explicit scheme within given } \Delta t}{\text{CPU time (sec) for implicit scheme within } \Delta t = 15 \text{ sec}}$$

for several 5-min simulations performed on the CRAY-1. In calculation of R_{CPU}, the initialization time (for input of coefficients, etc.) has been subtracted out to allow fair comparison of the Euler method with the two-step implicit scheme. In the

TABLE III

Computer Processing Time Ratios for Comparison of Explicit and Implicit Schemes

Δt (sec) (Euler Method)	R_{CPU} (a) (without $\lambda_{\mathscr{D}}$ calculation)	R_{CPU} (b) (with $\lambda_{\mathscr{D}}$ calculation)
1	5.21	5.75
2	2.62	3.20
6	0.86	1.27

simulations, the explicit scheme has been implemented (a) without eigenvalue calculation and (b) with calculation of $\lambda_{\mathscr{D}}$ at intervals of 30 sec in t. The two columns for R_{CPU} show the results for the two sets of simulations. When there is no eigenvalue calculation, it is seen that the explicit scheme with $\Delta t = 6$ sec is slightly faster than the implicit scheme. When the $\lambda_{\mathscr{D}}$ calculation accompanies the Euler method, as it would in practical application, the results favor the implicit method in all cases tested. For the case in which the explicit scheme requires a 1-sec time increment (e.g., the case in which $N_{00} = 2 \times 10^{-3}$, $R = 200$ mm hr^{-1}), the implicit scheme is nearly 6 times faster.

5. Summary

An implicit scheme has been designed for solution of the coalescence/collision-breakup equation. The scheme provides convergence without practical restriction on the step size and offers efficiency by requiring only the solution of (usually two) linear, uncoupled systems at each step. The allowed use of large time increments eliminates the need to incorporate temporal grid nesting in the design of moist convection models of meteorology. Such models entail solution of the microphysics equations at each spatial grid point within the domain of convective activity. In this context, the simplicity of the new scheme offers considerable advantage.

Acknowledgments

This work was supported by the Division of Atmospheric Sciences, National Science Foundation under Grant ATM-8113221. Computer support was provided by the National Center for Atmospheric Research which is sponsored by the National Science Foundation. The manuscript was prepared by Marjorie Northrop and Margaret Atticks.

References

1. P. S. Brown, Jr., *J. Atmos. Sci.* **28** (1971), 72.
2. P. S. Brown, Jr., *J. Atmos. Sci.* **38** (1981), 2758.
3. P. S. Brown, Jr., *J. Atmos. Sci.* **33** (1976), 1375.
4. J. R. Gillespie and R. List, *Pure Appl. Geophys.* **117** (1978), 599.
5. J. D. McTaggart-Cowan and R. List, *J. Atmos Sci.* **32** (1975), 1401.
6. Z. Levin, M. Neiburger, and L. Rodriguez, *J. Atmos. Sci.* **30** (1973), 944.
7. D. M. Whelpdale and R. List, *J. Geophys. Res.* **76** (1971), 2836.
8. A. C. Best, *Quart. J. R. Meteorol. Soc.* **76** (1950), 302.
9. R. Bleck, *J. Geophys. Res.* **75** (1970), 5165.
10. E. F. Danielsen, R. Bleck, and D. A. Morris, *J. Atmos. Sci.* **29** (1972), 135.
11. R. List and J. R. Gillespie, *J. Atmos. Sci.* **33** (1976), 2007.
12. P. S. Brown, Jr., *J. Climate Appl. Meteorol.* **22** (1983), 693.
13. T. Takahashi, *J. Atmos. Sci.* **34** (1977), 1773.
14. T. Takahashi, *J. Atmos. Sci.* **35** (1978), 1549.
15. L. Fox, "Numerical Solution of Ordinary and Partial Differential Equations," Addison–Wesley, Reading, Mass., 1962.
16. L. Fox, "An Introduction to Numerical Linear Algebra," Oxford Univ. Press, New York, 1965.
17. C. W. Gear, "Numerical Initial Value Problems in Ordinary Differential Equations," Prentice–Hall, Englewood Cliffs, N. J., 1971.